PERFORMANCE OF A SUPERCONDUCTING CAVITY STABILIZED RUBY MASER OSCILLATOR

D. M. Strayer and G. J. Dick,
Jet Propulsion Laboratory,
California Institute of Technology;
4800 Oak Grove Dr.
Pasadena, Ca. 91109

and J. E. Mercereau,
California Institute of Technology
1201 E. California Blvd.
Pasadena, Ca. 91125

Abstract

We first described an all-cryogenic oscillator system at the 1982 Applied Superconductivity Conference in Knoxville. This oscillator consists of a ruby cavity maser stabilized by a high-Q superconductor-on-sapphire resonator. The maser provides gain with very low noise and small power dissipation, while the sapphire substrate's thermal coefficient of expansion is 100 times smaller than that of superconducting metals. Having tested the major components and proved them satisfactory to the design, we have now assembled the first such oscillator and tested its performance in several preliminary configurations. The results of stability tests in a more advanced configuration will be reported. We shall describe this oscillator and shall report on its performance as a high-stability frequency source.

Introduction

An oscillator consisting of a ruby cavity maser stabilized by a high-Q superconducting cavity is being developed as a stable frequency source. Since our first description of this all-cryogenic oscillator at the ASC '82 meeting[1] the design has been refined sufficiently to warrant updating the description here. Several results important to the design have been measured and their implications to the expected oscillator performance will be related. Tests of stability have been made in several configurations of the oscillator en route to an optimum system configuration. These results will be discussed with consideration of the adjustments required to improve the stability of the oscillator.

While many groups have worked to develop oscillators stabilized by superconducting cavities, we shall cite a few whose work has provided building blocks for the present effort. Stein and Turneaure[2] built a system using a niobium cavity and room temperature electronics, obtaining the best oscillator stability ever reported. Their results actually inspired our interest in this area.

Manuscript received September 30, 1986.

Braginsky and coworkers at Moscow discussed[3] and later demonstrated[4] the advantages of a cavity formed by depositing a superconducting film on a sapphire substrate. More recently, Braginsky and coworkers[5] and separately Blair and his coworkers[6], have proposed employing an uncoated sapphire dielectric resonator as a stabilizing cavity, a scheme that interests us for certain applications.

Components

The prototype oscillator now being tested is designed to obtain stability levels of one part in 10^{15} at measuring times longer than 1000 seconds. The major components, the superconducting cavity and the ruby maser, must attain some minimum performance to allow this stability level to be achieved. We have characterized these components in preliminary tests, and these measurements will be described here.

Several aspects of the cavity performance are relevant to the oscillator stability. Any change of the cavity resonance frequency will be reflected directly in a change in the oscillator frequency, so the most stable cavity possible is desired. The high Debye temperature of sapphire combined with its high strength make a sapphire cavity substrate a likely choice for reducing cavity response to perturbations such as temperature drifts, tilt and vibrations. However, such stability must not be obtained at the cost of high Q in the cavity. Our measurements of the Q of cavities formed by evaporating a Pb film onto a cylindrical sapphire substrate have yielded values exceeding 2×10^9 at a temperature of 1.5 Kelvin.[7] (See Fig.1) This low signal absorption will facilitate achieving the oscillator stability goal.

Figure 1 shows the results of measurements of the quality factor of a Pb-on-sapphire cavity in three different setups. For the first set (Run 1 in the figure), the Pb-on-sapphire cavity was placed inside a Pb-on-copper cavity whose Pb film was several months old. The second set of data (Run 2) was obtained with the Pb-on-sapphire cavity mounted in a bare copper cavity, while the third was obtained with it inside a newly plated Pb-on-copper cavity. Since the bare copper cavity would itself not be expected to give Q-values greater than 10^5, the measured Q of 3×10^8 shown for the second run indicates that the Pb-on-sapphire resonator is isolated from the containing cavity by a factor of at least 3000. This isolation implies that the small differences in the data of the first and

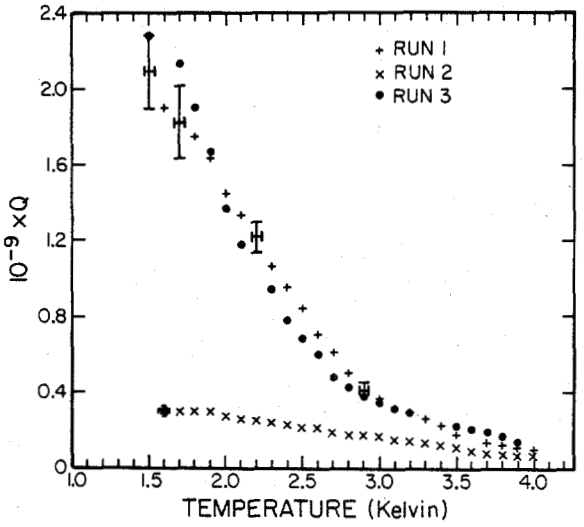

Figure 1. Measured Q values for the lead-on-sapphire cavity during three different cooldowns. Experimental conditions described in text.

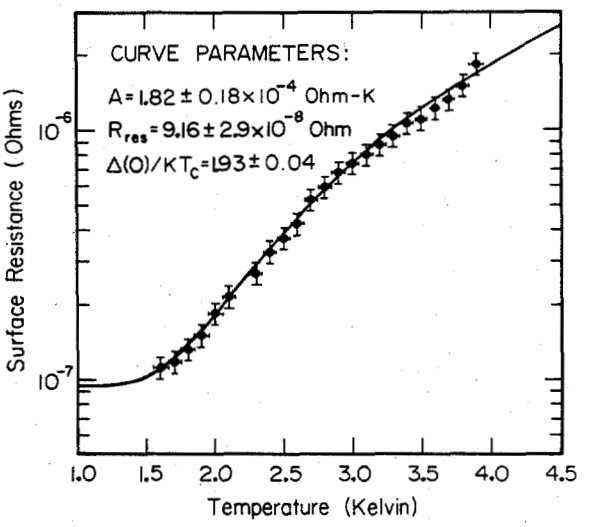

Figure 2. Surface resistance values derived from runs of previous figure. The curve represents Eq.(2) fitted to the data with parameters as indicated in the figure.

third runs are not caused by differences in the quality of the lead films on the containing cavity. Note that no systematic reduction of the cavity Q occurs with successive cooldowns, contrary to results for Pb films reported by others.[5]

These Q measurements can provide surface resistance values for the Pb film by the relation

$$Q \times R_s = G \qquad (1)$$

where G, 255 ohms, is the geometric factor for the cavity. Values of surface resistance derived from the third run of Fig.1 are shown in Fig. 2. Also shown is a curve that was fit to the date using the relation

$$R_s = R_{res} + \left(A/T\right) \exp\left[-\Delta(T)/kT\right] \qquad (2)$$
$$= R_{res} + R_{BCS}(T)$$

This formula for R_s shows the separation into a temperature independent "residual resistance" R_{res} and a temperature dependent surface resistance R_{BCS} predicted by the Bardeen-Cooper-Schrieffer theory of superconductivity[8]. The temperature dependence of the energy gap $\Delta(T)$ has been approximated as described by Sheahen[9]. In the curve fitting, R_{res}, A and $\Delta(0)$ were all allowed to vary.

The results of the fitting are shown on Fig. 2. They are significant in that the energy gap and residual resistance obtained are typical of values derived by other workers for thin Pb films[10]. The residual resistance is smaller than that measured for other evaporated Pb films[4,11], so any damage or contamination effects occurring at the Pb film interface to the sapphire would appear to be small.

Ruby maser amplifiers are known to have very low noise temperatures, but the use of rubies in oscillators had not been studied before our own work. We have looked for frequency fluctuations caused by the ruby in oscillators utilizing low-Q cavities (to allow these fluctuations to be readily measured). We find that with a cavity Q of 1100 the frequency fluctuations due to all sources[12] are approximately $df/f \sim\sim 10^{-10}$. This measurement places an upper limit to the multiplicative 1/f phase noise in the active ruby of -135db/f. We believe this to be the lowest value ever measured for an active microwave device, and is comparable to the best available passive devices. For comparison, while the noise figure of GaAsFET transistors improves dramatically at low temperatures, their multiplicative 1/f noise is apparently not reduced. GaAsFET's designed for oscillator service show 1/f noise values from -80db/f to -95db/f depending on frequency, with bipolar devices perhaps 15db better, but showing higher noise temperature than cooled FET's.

In a more direct extrapolation, improving the cavity Q only to 1.1×10^9 would allow frequency fluctuation levels of 10^{-15} to be achieved. Because the instabilities observed at longer times in this low-Q system were caused by elements such as coupling probes rather than by the ruby, we expect with the high-Q cavity described above to be able eventually to obtain stabilities well below the 10^{-15} goal we have set for this prototype oscillator.

With a measured noise temperature below 3K in amplifier service[13], the ruby maser represents the quietest active device available for a cryogenic oscillator. A continuous output power of more than 10nW can be achieved with dissipation to the Helium bath of only 10 microwatts. Figure 3 shows the consequences of these device parameters on oscillator performance.

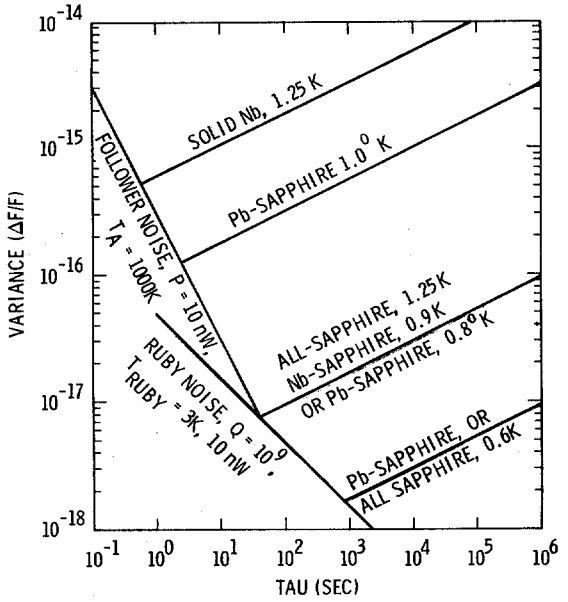

Figure 3. Performance capability of the SCM for various stabilizing cavity technologies and operating temperatures.

Oscillator Design

Successful design of a stable oscillator combining the ruby maser and a superconducting cavity requires that microwave fields be coupled between them in such a way that the oscillations generated in the ruby are stabilized by the effect of the cavity. At the same time, the 0.05 Tesla bias field required for operation of the maser must be isolated from the cavity to prevent degradation of its Q. We have chosen to use a 3/2 wavelength coaxial resonator as an intermediate element to provide the requisite coupling and isolation. We have also chosen to operate the ruby in its own coaxial resonator to allow characterization and optimization of the ruby itself independent of the operation of the stabilized oscillator.

The three coupled cavities as shown in Figure 4 form a multiply resonant system, one mode of which provides appropriately stabilized operation, the other two modes being designed in such a way that they do not oscillate. Analysis of the design is complicated by the fact that the modes in the various parts of the system are of different sorts; the ruby and coupling resonators are excited in coaxial TEM modes, while the stabilizing resonator uses a TE_{011} mode for high Q. It is possible, however, to design all operational aspects of such an oscillator without detailed knowledge of the internal fields, since these aspects follow uniquely from the resonator frequencies, coupling constants, and Q's. A description of the method used to calculate the frequencies and Q's for each mode of the oscillator has already been presented.[12] This process has now been inverted to allow resonator frequencies and coupling constants to be inferred from given requirements on mode Q.

Of particular significance to the design process are the relative energy contents of the three cavities in the stabilized mode.

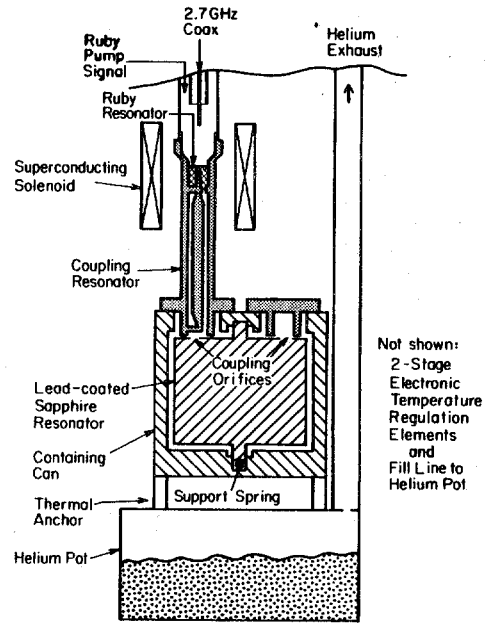

Figure 4. Schematic diagram of three-cavity superconducting maser with a super-conductor-sapphire stabilizing resonator.

Given the Q of the stabilizing resonator and the (negative) value for that of the pumped ruby resonator, the condition of power balance determines a minimum fractional energy content in the ruby resonator for oscillation. Since this fraction also represents the sensitivity of the mode frequency to that of the ruby resonator, all such pulling effects can be shown to scale with the Q of the stabilizing resonator.

The general features of the mode selection process can be understood from Figure 5. The resonant frequencies of the coupled cavity system, ω_α, ω_β and ω_γ, represent modes with energy principally in the ruby, coupling, and stabilizing cavities. Each mode actually has some energy in each of the three physical resonators, and the tendency of a given mode to oscillate is enhanced by its Q, by the fraction E_r/E of its energy in the pumped ruby resonator, and by the (negative) Q of the ruby at the mode frequency. All other things being equal, oscillation will

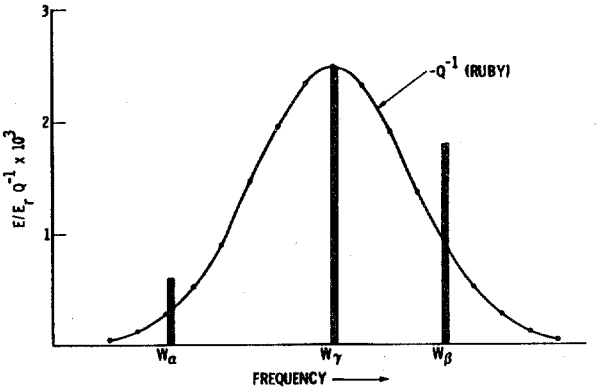

Figure 5. Mode selection graph. Ruby gain compared to mode loss for a coupled 3-resonator system.

naturally occur first in the mode with most of its energy in the ruby-filled resonator. This mode of oscillation must be suppressed and instead, the stabilized mode, with nearly all of its energy in the sapphire resonator, must be excited.

The frequency dependence of the regenerative power of the ruby, shown as the solid curve in Figure 5, allows selection of this desired mode. Operation in the unwanted modes is prevented by requiring that their frequencies lie sufficiently far from that of the stabilized mode so that, even though their Q's are enhanced, mode losses overcome the ruby's regenerative power. As illustrated, te center frequency of the ruby gain is tuned to the stabilized mode by adjustment of the magnetic bias field, giving oscillation in that mode. The frequencies of the other modes have been adjusted so that their Q's are just doubled.

The method used to tune and couple the three resonators in order to obtain the desired energy balance in the stabilized mode has been previously discussed.[12] Figure 6 shows the relationship of resonator frequencies, labeled 1, 2, and 3, and mode frequencies, labeled alpha, beta, and gamma. Construction of the stabilized mode was accomplished by the use of the eigenfrequency diagram shown in c), and the relationship

$$\omega_{ij} = \gamma_{ij}\sqrt{E_j/E_i} \qquad (3)$$

as derived in reference 12. Here, γ_{ij} represents the coupling strength in units of frequency between the resonators i and j, and the sign depends on the nature of the coupling and relative phase between them. In this perspective, the construction of a mode of the system is accomplished by arranging for all of the individual resonators in the system to tune each other to the same frequency.

We have chosen to construct a first model of the stabilized oscillator with the ruby and coupling cavities made of OFHC copper as depicted in Figure 4. While mechanical stabilities in these devices is much poorer than that of the sapphire, their low energy content, made possible by the high Q of the stabilizing resonator, allows us to project stability of 10^{-16} for this device.

Results

Even though the Q of the stabilizing resonator is greater than 10^9, the Q of the stabilized mode can be much lower, without maser activity, depending on the energy content of the low Q copper resonators. Such a low-performance condition is appropriate for system development and debugging, however, since a relatively large energy content in the ruby ensures a capability for oscillation in the stabilized mode. As discussed above, frequency pulling effects are also proportionately increased, and so variations of the output frequencies due to the maser pump signal and bias field, being larger, are more easily characterized.

a)

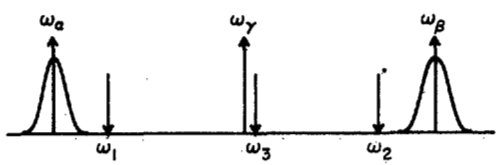

b)

Mode →	α	γ	β
E_1^η	0.85	$1/2\times10^{-5}$	0.15
E_2^η	0.15	$1/2\times10^{-5}$	0.85
E_3^η	$.8\times10^{-6}$	≈ 1	$.4\times10^{-5}$

c)

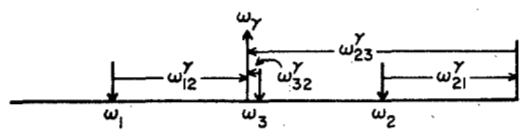

Figure 6. a) Frequency response of a three-cavity resonator. Response bandwidth of the high Q mode is not shown. Cavity frequencies and eigenfrequencies are identified.
b) Table of fractional energy in each cavity for the three modes.
c) Eigenfrequency diagram for the high-Q mode.

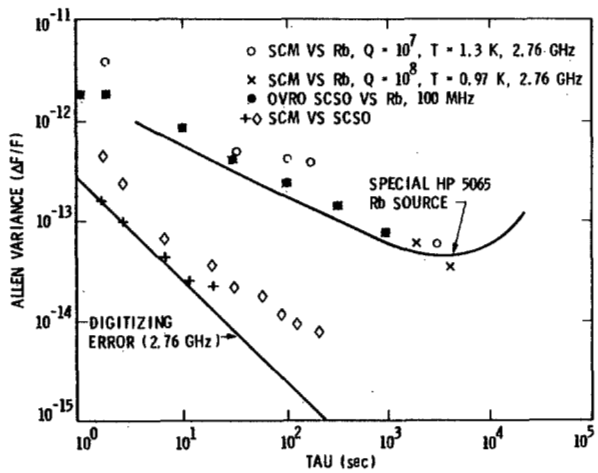

Figure 7. Performance of the Superconductive Cavity Maser using Rb and SCSO frequency sources for reference.

The oscillator stability performance in several configurations is shown in Figure 7. The Allen variance is formed by repeatedly measuring the frequency, then finding the difference from the previous measurement, and calculating the variance of these differences.[14] As indicated, this value is normalized by dividing by the oscillator frequency itself. The horizontal axis is the measuring time tau used for each frequency measurement. The solid curve represents the stability performance of a good rubidium frequency source. We have in our laboratory a superconducting cavity stabilized oscillator (SCSO) of the Stein-Turneaure type that we use to compare to our oscillator.

Note that the figure shows that both the SCSO and our superconducting cavity maser (SCM) oscillator trace out the rubidium curve when measured with our stability characterizing system.[15] The solid straight line on Fig. 7 represents the estimated limit of stability that can be characterized by this system.

Two runs of data are shown for a comparison of our SCM to the SCSO.[8] In both runs, the SCM mode Q was 10^8 and its operating temperature was near 1.0K. The stability is at the limit of the measuring system for very short measuring times. The best stability shown, 8×10^{-15} at 256 seconds measuring time, is characteristic of the SCM, since this SCSO has demonstrated 3×10^{-15} stability at this measuring time.

These results are near the design goal of 10^{-15} stability for this oscillator. Just as important to the development of improved versions are the results of frequency response to various perturbations of the oscillator system. In particular, we have found a significant change of frequency with change of amplitude of the RF pump signal. Also, the response to temperature change is anomalously large. Reaching 10^{-15} stability requires only slightly better stabilization of these two parameters combined with higher mode Q. However, to reach 10^{-17} stability in future versions of the SCM will require either reduction of the response to these perturbations or more sophisticated stabilization techniques.

Acknowledgments

The authors gratefully acknowledge the assistance of Nils Asplund in this work. The research described in this paper was carried out at the Jet Propulsion Laboratory and at the Low Temperature Laboratory of the California Institute of Technology with support from the Jet Propulsion Laboratory, which is under contract to the National Aeronautics and Space Administration.

References

1. D. M. Strayer, G. J. Dick and E. Tward, IEEE Trans. Magnetics MAG-19, 512, 1983.

2. S. R. Stein and J. P. Turneaure, Proc. 27th Ann. Freq. Control Symp., USAERADCOM, Ft. Monmouth, N.J., 414, 1975. Also, S. R. Stein and J. P. Turneaure, Proc. Conf. on Future Trends in Superconductive Electronics, AIP Conf. Proc. No. 44, 192, 1978.

3. V. B. Braginsky and V.I. Panov, IEEE Trans. Magnetics MAG-15, 30, 1979.

4. V. B. Braginsky, V.I. Panov and S.I. Vasiliev, IEEE Trans. Magnetics MAG-17, 955, 1981.

5. V. B. Braginsky, V.P. Mitrofanov and V.I. Panov, Systems with Small Dissipation (Univ. of Chicago Press, Chicago, 1985), 85-89; Frequency Stabilization of oscillators with high-Q leucosapphire dielectric resonators, V. I. Panov and P. R. Stankov, Radiotekhnika i Electronika 31, 213, 1986,(In Russian).

6. D. G. Blair and S. K. Jones, IEEE Trans. Magnetics MAG-21, 142, 1985.

7. S. Thakoor, D. M. Strayer, G.J. Dick and J.E. Mercereau, J. Appl. Phys. 59, 854, 1986.

8 J. Halbritter, Z. Phys.243, 201, 1971.

9. Thomas P. Sheahen, Phys. Rev. 149, 368, 1966.

10. T. Yogi, Ph.D. thesis, California Institute of Technology, 1977.

11. P. Flecher, Externer Ber 3, 70-5, 1970; P. Flecher, J. Halbritter, R. Heitschold, P. Kniesel, W. Kuhn and O. Stoltz, IEEE Trans. Nucl. Sci. NS-16, 1018, 1969.

12. G. J. Dick and D. M. Strayer, Proc. 38th Ann. Freq. Control Symp. (Elec. Industries Assoc., 1984), 414.

13. J. V. Jelly, Proc. IEEE 51, 30, 1963. Also, R.C. Clauss, Jet Propulsion Laboratory, California Institute of Technology, Pasadena, Ca., private communication.

14. J. A. Barnes, R. Chi, L.S. Cutler, D. J. Healey, D.B. Leeson, T.A. McGunigal, J.A. Mullen, Jr., W.L. Smith, R.L. Sydnor, R.F.C. Vessot, and G.M.R. Winkler, IEEE Trans. Instr. and Meas. IM-20, 105, 1971.

15. D. M. Strayer, G. J. Dick and J. E. Mercereau, to be published in Proc. 17th Ann. Precise Time and Time Interval Application and Planning Meeting, 1985.